Specific Mutations Alter Fibrillation Kinetics, Fiber Morphologies, and Membrane Interactions of Pentapeptides Derived from Human Calcitonin

3 AUTHORS, INCLUDING:

Tania Sheynis
University of Leeds
25 PUBLICATIONS **418** CITATIONS

Specific Mutations Alter Fibrillation Kinetics, Fiber Morphologies, and Membrane Interactions of Pentapeptides Derived from Human Calcitonin

Amit Shtainfeld, Tania Sheynis, and Raz Jelinek*

Department of Chemistry, Ben Gurion University of the Negev, Beer Sheva 84105, Israel

Received February 23, 2010; Revised Manuscript Received May 18, 2010

ABSTRACT: Protein misfolding and fibrillation are fundamental facets underlying a diverse group of amyloid disorders and diseases. The molecular factors responsible for amyloid protein toxicity and pathological consequences, however, are still not fully understood. The involvement of specific residues or sequence elements in fibril formation and the interactions of amyloid protein aggregates with membranes are believed to constitute two critical parameters contributing to amyloidogenesis and amyloid pathologies. This work aims to elucidate sequence determinants and membrane−protein interactions of five-residue peptide fragments derived from a core amyloidogenic sequence of human calcitonin. We show that single-residue mutations within the native pentapeptide sequence significantly modulate the kinetics of peptide self-assembly, alter β-sheet organization between parallel and antiparallel arrangements, and modify fibrillar morphologies. We further demonstrate that hydrophobic or aromatic interactions are not prerequisites for peptide fiber formation. The experiments also disclose pronounced effects of lipid vesicles comprising cholesterol and negatively charged phospholipids on the rate of fibrillation and fiber structures formed by the short peptides. This work indicates that the structural and kinetic properties of peptide fibrils as well as lipid interactions of fibrillar species are interrelated and are significantly affected by specific residues within amyloid peptide sequences.

The transformation of soluble proteins into amyloid fibrils deposited in different organs and tissues is a hallmark of varied medical disorders, including Alzheimer's disease, Parkinson's disease, type II diabetes, and others. While many amyloid-forming proteins do not share sequence homologies, the deposits that are being formed exhibit similar structural characteristics, including an unbranched filamentous appearance and cross-β-sheet motifs (*1, 2*). General physicochemical properties associated with the polypeptide sequence, such as hydrophobicity, net charge, and propensity to form a β-sheet are believed, to significantly affect kinetics of amyloidogenesis and fibril structures (*3−6*). In particular, the alternating organization of hydrophobic and hydrophilic amino acids was found to be a primary structural element contributing to acceleration of the peptide fibrillation (*5, 7*). Such patterns facilitate protein self-assembly by preserving the amphipathic topology of parallel β-sheet arrangements (*8*). In addition, the abundance of aromatic residues within the peptide sequence was predicted theoretically (*9*) and shown experimentally (*10*) to increase the rate of fibril formation.

Aggregation of amyloid proteins frequently results in fibrils bearing distinct shapes and structural modes, even for deposits consisting of the same molecule (*11−13*). External conditions, including agitation, pH, and traces of fluorinated solvent, can affect structural features of the resulting filaments (*14, 15*). Intriguingly, β-amyloid fibrils displaying specific morphologies were shown to exhibit toxic properties (*14*). Certain chemical compounds were also shown to modify the morphological properties and toxicity of amyloid aggregates (*16−18*). A very limited number of reports, however, link specific mutations within

protein sequences to the formation of distinct fibrillar structures and their biological significance. Naturally occurring mutations in the α-synuclein sequence (*19*) and substitution of aromatic amino acids in the islet amyloid polypeptide (*10*) were shown to induce only mild morphological changes in fibrils of the respective proteins.

Beside the contribution of specific structure elements and residues to amyloidogenesis, there is growing evidence that lipid and membrane interactions play significant roles in the progression and toxicity of amyloid diseases (*20−22*). Investigations of amyloid protein systems have determined that specific lipid components such as "lipid rafts" promote amyloid fibril formation and the deposition of plaques on membrane surfaces (*23−25*). A growing body of experimental evidence appears to indicate that oligomeric species formed in early stages of aggregation, rather than mature full-length fibrils, are responsible for amyloid-induced cytotoxicity (*26−30*). Nevertheless, there have been intriguing reports about amyloidogenic peptides such as SEVI for which the aggregated amyloid assembly was membrane active (*31*). Other peptides, such as IAPP1−19, were shown not to form fibrils but were still toxic (*32*).

Human calcitonin (hCT) is a 32-residue peptide hormone that plays an important role in calcium metabolism and, further, possesses a number of other biological activities (*33*). Calcitonin exhibits a marked tendency to form amyloid fibrils, which have been identified both in vivo (*34*) and in vitro (*35*). Previous studies have revealed prominent contributions of membrane interactions toward calcitonin fibrillation (*36*) and indicated formation of calcitonin-induced oligomeric pores in lipid bilayers (*37*). Moreover, it was shown that incubation of calcitonin with ganglioside- and cholesterol-rich membranes resulted in pronounced amyloidogenic structures (*38*). Previous investigations demonstrated

*To whom correspondence should be addressed. E-mail: razj@bgu.ac.il. Telephone: +972-8-6461747. Fax: +972-8-6472943.

that very a short peptide fragment of hCT, comprising five amino acids, could assemble into amyloid fibril structures that were highly similar to the parent hCT protein (*39*). In general, characterizing the fibrillation properties of short peptides or fragments of larger amyloidogenic proteins is important since such studies illuminate the contributions and significance of specific residues (or short sequence elements) to the fibrillation phenomena (*40*, *41*).

This study aims to investigate the impact of specific mutations on fibrillar morphology, aggregation rate, and membrane interactions of DFNKF, a peptide fragment spanning residues 15−19 of hCT. Two substituted analogues of this pentapeptide were studied: DANKA (the phenylalanines substituted with alanines) and DFNMF (lysine substituted with methionine). Via a comparative analysis of the native sequence and the two mutants, the roles of the aromatic phenylalanine residues and the positively charged lysine in fibrillation and membrane interactions were elucidated. The experiments were also designed to evaluate the contribution of specific lipid bilayer constituents to fibrillation of the short peptides. The experimental results point to remarkable effects of the mutations upon the fibrillar structures and rate of fibril formation and highlight the close relationships among amino acid sequence, lipid interactions, and fibrillation phenomena.

MATERIALS AND METHODS

Materials. 1,2-Dimyristoyl-*sn*-glycero-3-phosphocholine (DMPC); 1,2-dimyristoyl-*sn*-glycero-3-[phospho-*rac*-(1-glycerol)] (DMPG); cholesterol; 1,2-dipalmitoyl-*sn*-glycero-3-phosphoethanolamine *N*-(7-nitro-2−1,3-benzoxadiazol-4-yl), ammonium salt (NBD-PE); and 1,2-dipalmitoyl-*sn*-glycero-3-phosphoethanolamine *N*-(lissamine rhodamine B sulfonyl), ammonium salt (rhodamine-PE), were purchased from Avanti Polar Lipids (Alabaster, AL). Peptide synthesis was performed by Peptron, Inc. (Taejeon, Korea). The integrity of the peptides was confirmed by ion spray mass spectrometry, and their purity (at least 90%) was determined by reverse phase high-pressure liquid chromatography.

Vesicle Preparation. We prepared small unilamellar vesicles (SUVs) consisting of DMPC and cholesterol (7:3 molar ratio) or DMPC, DMPG, and cholesterol (7:2:3 molar ratio) by dissolving all lipid components in chloroform/ethanol mixtures (1:1, v/v) and drying them together in vacuo to a constant weight. Dry lipid films were suspended in 10 mM Tris base (pH 7.2), 10 mM NaCl, and 0.02% NaN_3 by probe sonication at room temperature for 10 min, yielding a total lipid concentration of 1 mM. Vesicle suspensions were allowed to anneal for 1 h prior to use.

Peptide Samples. Stock solutions of the peptides were prepared by dissolving lyophilized samples in DMSO at a concentration of 100 mg/mL. The stock solutions were diluted with 10 mM Tris base (pH 7.2), 10 mM NaCl, and 0.02% NaN_3, mixed with vesicles (final lipid concentration of 0.5 mM) or with an equal volume of the aforementioned Tris buffer, and incubated at 26 °C without agitation. Final peptide concentrations of DFNKF and DANKA were 4 mg/mL, and that of DFNMF was 0.5 mg/mL. For control samples, pure DMSO was used instead of peptide stocks. Aliquots were withdrawn from the samples at the indicated time points and used for all experiments. Blocked Eppendorf tubes were used for incubation of the peptide solutions. The blocking was performed by shaking the tubes in a 3% skim milk powder dissolved in PBS (10 mM, pH 7.4) for 3 h at 37 °C. Subsequently, the tubes were washed under running distilled water and dried.

Transmission Electron Microscopy (*TEM*). Fibril formation was assessed using 5 μL of the peptide samples placed on 400 mesh copper grids covered with a carbon-stabilized Formvar film. Following a 2 min incubation, excess solutions were removed and the grids were negatively stained for 1 min with a 1% uranyl acetate solution. Samples were viewed with a JEOL 1200EX electron microscope operating at 120 kV.

Congo Red (*CR*) *Staining and Birefringence*. Aliquots (10 μL) of peptide solutions in buffer or peptide/vesicle suspensions incubated for 6 h were allowed to dry on a glass microscope slide. Staining was performed by the addition of 80% ethanol saturated with Congo Red and NaCl. Birefringence was determined with a SZX-12 Stereoscope (Olympus, Hamburg, Germany) equipped with a polarizing stage.

Fourier Transform Infrared Spectroscopy (*FTIR*). Peptide solutions in buffer and peptide/vesicle suspensions were completely dried under vacuum for several days. KBr pellets were prepared from 2.0 mg of a well-dried sample mixture and 120.0 mg of dried KBr. FTIR was conducted using a FTIR 460 Plus spectrophotometer (Jasco, Tokyo, Japan). IR spectra were recorded at a resolution of 2 cm^{-1} in the range of 400−4000 cm^{-1}.

Fluorescence Resonance Energy Transfer (*FRET*). Lipid vesicles were prepared by the procedure described above. Prior to being dried, the lipids were additionally supplemented with NBD-PE and rhodamine-PE at a 100:1:1 molar ratio. At selected time points, 15 μL aliquots were withdrawn from the peptide/vesicle mixtures and diluted with deionized water to 0.5 mL, and fluorescence emission spectra were recorded on a FL920 spectrofluorimeter, applying an excitation wavelength of 469 nm. The percentage of FRET efficiency was determined by the equation

$$\% \, \text{FRET efficiency} = 100\% \times (R_i - R_{0\%})/(R_{100\%} - R_{0\%})$$

where R is a ratio of fluorescence emission of rhodamine-PE (590 nm) to that of NBD-PE (536 nm), R_i indicates the ratio for peptide/vesicle mixtures, $R_{0\%}$ was measured following the addition of 10% Triton X-100 to the vesicles (Triton X-100 is a detergent causing complete dissociation of the vesicles), and $R_{100\%}$ corresponds to vesicles without any additives. The percent FRET efficiency of control samples prepared by addition of only DMSO to vesicles was subtracted from the corresponding values recorded for the peptide/vesicle solutions.

RESULTS

Previous studies have shown that very short peptides corresponding to sequence elements within human calcitonin (hCT) form fibrillar structures. The three peptides studied here are derived from residues 15−19 of hCT, a short fragment believed to play a primary role in aggregation of the protein (*39*). DFNKF is the native sequence, containing two phenylalanine residues thought to be intimately involved in the fibrillation of the full-length peptide (*39*). The two phenylalanines were substituted with alanines in DANKA, while lysine was substituted for methionine in DFNMF, designed to evaluate the significance of the positively charged lysine in fibrillation and membrane interactions.

Figure 1 depicts transmission electron microscopy (TEM) images that illuminate the kinetics and morphologies of fibril aggregates formed by the three peptides, and the relationship between peptide fibrillation and the presence in the incubation solution of lipid bilayers comprising dimyristoylphosphatidylcholine (DMPC), dimyristoylphosphatidylglycerol (DMPG),
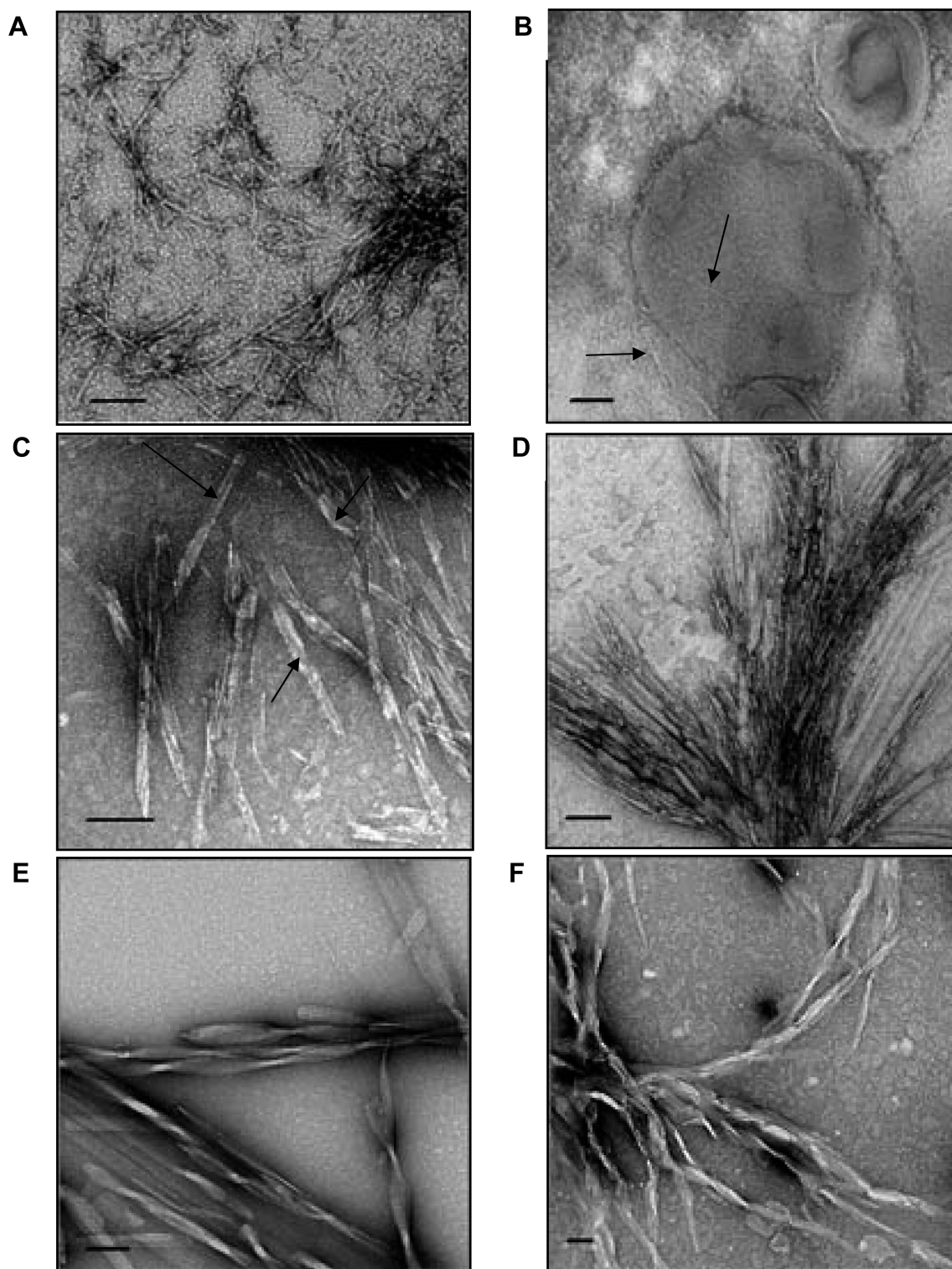
FIGURE 1: Fibrillation of pentapeptides in buffer and in lipid vesicle solutions. TEM images showing the structures of peptide aggregates formed. DFNKF (4 mg/mL) (A) in buffer (6 h incubation) and (B) in a DMPC/DMPG/cholesterol vesicle solution (1 h) (arrows point to fibrils). DANKA (4 mg/mL) (C) in buffer (1 h) (arrows point to hollow fibrils) and (D) in a DMPC/DMPG/cholesterol vesicle solution (1 h). DFNMF (0.5 mg/mL) (E) in buffer (3 h) and (F) in a DMPC/DMPG/cholesterol vesicle solution (1 h). The bars correspond to 100 nm.

and cholesterol. This vesicle composition is designed to mimic physiological membranes; thus, the vesicles comprise representative phospholipids displaying zwitterionic (PC) and anionic (PG) headgroups, as well as cholesterol, which is abundant in the plasma membrane of human cells (*42, 43*).

The TEM data in Figure 1 demonstrate that all three peptides form fibrillar structures, albeit exhibiting significantly different structures. Furthermore, the TEM experiments reveal that the

DMPC/DMPG/cholesterol vesicles modulated both the aggregation kinetics of the peptides and the structural features of the fibril assemblies formed. However, different effects of the vesicles were apparent among the peptides. Interestingly, even though clear fibril structures were observed in the TEM experiments summarized in Figure 1, no thioflavin-T (ThT) fluorescence signals were observed when this fibril marker dye was added to the peptide solutions (data not shown), possibly due to the short sequences.

The native sequence DFNKF formed elongated thin fibrils in buffer which exhibit morphologies comparable to the fibrillar structures of full-length calcitonin (*35*) (Figure 1A). The DFNKF fibrils appeared in buffer solutions only after approximately 6 h (Figure 1A), while abundant fibrillation occurred less than 1 h after dissolution of the peptide in lipid vesicle solutions (Figure 1B). Structurally, the DFNKF fibrils formed in the presence of vesicles (Figure 1B, fibrils indicated by the arrows) appear to be similar to those formed in the lipid-free buffer solution (Figure 1A).

DANKA, in which the phenylalanine residues were substituted with alanines, also formed elongated aggregates (Figure 1C,D). However, the morphologies and kinetics of the DANKA fibers were different from those of the native sequence. Specifically, fibrillar structures of DANKA were clearly apparent after 1 h, both in the buffer solution (Figure 1C) and in the presence of DMPC/DMPG/cholesterol vesicles (Figure 1D). The lipid vesicles seem to have induced thicker "bundles" of DANKA fibers (Figure 1D), although the individual fiber morphologies seem to be similar to those observed in the vesicle-free buffer solutions (Figure 1C). The apparent hollow and semifragmented tubular structures of the DANKA fibers were markedly different from the long and thin fibrillar assemblies of the native fragment DFNKF (Figure 1A,B).

Distinct fibrillation profiles are apparent in the case of the lysine-to-methionine substituted sequence DFNMF (Figure 1E,F). In buffer, DFNMF assembled into fibrillar structures only after at least 3 h (Figure 1E). The DFNMF fibers formed in the vesicle-free solution were thicker than the native sequence (Figure 1A) and displayed distinct screwlike morphologies. In the presence of the DMPC/DMPG/cholesterol vesicles, however, DFNMF formed aggregates significantly faster [within less than 1 h (Figure 1F)]. The vesicle-induced fiberlike structures appeared fragmented and much more frayed than the fibrillar structures formed in the buffer solutions (Figure 1E). Furthermore, the twisted morphologies of the DFNMF fibers appear to be largely absent in the vesicle solutions. Overall, the TEM images in panels E and F of Figure 1 underscore the pronounced effect of the lipids upon the DFNMF fiber assemblies. Importantly, DFNMF formed fibrils at a much lower concentration (0.5 mg/mL) than the native DFNKF and the mutant DANKA sequences (4 mg/mL for both peptides). In fact, we found that when the concentration of DFNMF was increased to 4 mg/mL, fibrils formed immediately after dissolution of the peptide in buffer (data not shown). This remarkable increase in aggregation rate indicates an enhanced propensity of DFNMF for fiber assembly.

To assess the secondary structure of the fibrillar species formed by the three pentapeptides, we conducted Fourier transform infrared (FTIR) spectroscopy experiments (*44*). Figure 2 depicts the FTIR amide I region spectra of the fibrillar aggregates formed by the three peptides in the presence of the DMPC/DMPG/cholesterol vesicles. FTIR spectra which were highly similar to the results shown in Figure 2 were recorded for fibrils formed in buffer (data not shown), indicating that the lipid vesicles did not alter the short-range structural features of the fibrils.

The FTIR data in Figure 2 confirm that fibrillar species of all three peptides comprised β-sheet elements, giving rise to the distinctive peaks at $\sim$1670–1680 and $\sim$1620–1630 cm^{-1} (*45*). Interestingly, the FTIR signatures in Figure 2 demonstrate pronounced differences between the two *residue*-substituted peptides.
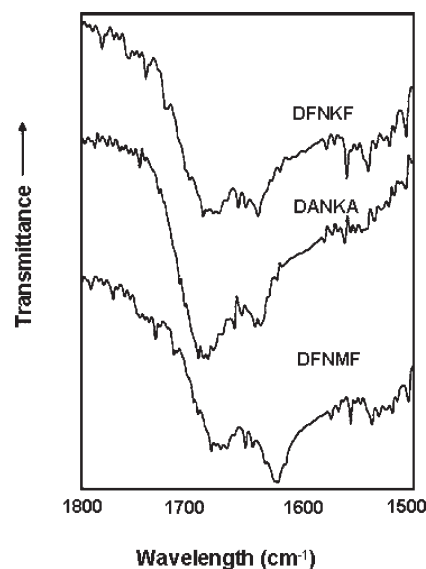

FIGURE 2: FTIR spectra. Spectra recorded for peptide samples incubated for 6 h in DMPC/DMPG/cholesterol vesicle solutions.

Specifically, while DANKA seems to predominantly adopt an antiparallel β-sheet organization, evident by the high intensity of the peak at $\sim$1680 cm^{-1} (*46, 47*), DFNMF mainly forms parallel β-sheet structure [more pronounced signal at 1630 cm^{-1} (*48*)]. This difference most likely reflects the absence of $\pi-\pi$ interactions in the DANKA fiber aggregates, which constitute a primary structure element controlling the arrangement of β-strands.

While FTIR experiments illuminate the extent of localized secondary structure elements (*44*), we additionally examined the peptide assemblies using Congo Red (CR) staining to analyze the amyloid nature of the fibrillar structures formed by the three pentapeptides and the effects of lipid bilayers upon amyloid deposit formation. Green-yellow birefringence of CR in cross-polarized light is considered a reporter for long-range β-cross structure which is a primary characteristic of amyloid fibrils (*49*). The cross-polarized optical microscopy images in Figure 3 point to differences in the macroscopic properties of the aggregates formed by the three peptides examined and particularly demonstrate the significant effects of the lipid vesicles on the peptide assemblies.

Specifically, while green-yellow regions, corresponding to amyloid fibril deposits, appeared in samples of the native sequence DFNKF that were incubated for 6 h either in buffer (Figure 3A) or with DMPC/DMPG/cholesterol vesicles (Figure 3B), no green-yellow birefringence was detected in samples of the two substituted peptides, DANKA and DFNMF, that were incubated in buffer (panels C and E of Figure 3, respectively). In contrast, incubation of both DANKA and DFNMF with DMPC/DMPG/cholesterol vesicles yielded amyloid fibril deposits, giving rise to the green-yellow CR domains observed in the optical microscopy images shown in Figure 3D (DANKA) and Figure 3F (DFNMF).

The microscopy and FTIR analyses in Figures 1–3 focus on the structural properties of the fibers formed by the three pentapeptides and the effects of lipid bilayers on the microscopic organization, morphologies, and molecular structures of the fibril assemblies formed. It is similarly important, however, to evaluate whether the fibrillar species formed in solution interact with and affect the properties of the lipid bilayers. Figure 4 presents fluorescence resonance energy transfer (FRET) experiments (*50*)
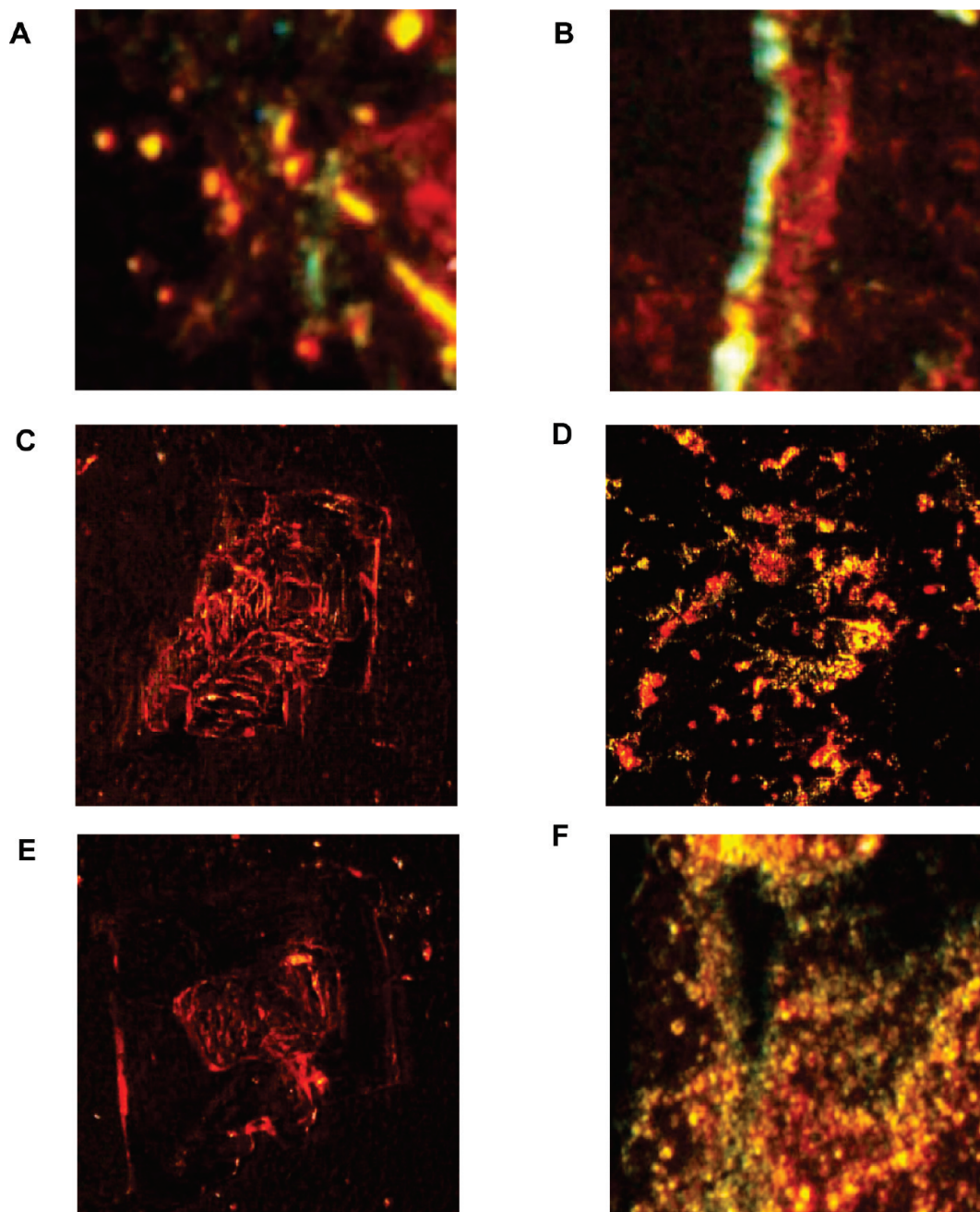
FIGURE 3: Amyloid fibril deposits examined by Congo Red birefringence. Optical images recorded for peptides incubated for 6 h. DFNKF (4 mg/mL) (A) in buffer and (B) in a DMPC/DMPG/cholesterol vesicle solution. DANKA (4 mg/mL) (C) in buffer and (D) in a DMPC/DMPG/cholesterol vesicle solution. DFNMF (0.5 mg/mL) (E) in buffer and (F) in a DMPC/DMPG/cholesterol vesicle solution.

conducted using two vesicle compositions: DMPC/cholesterol and DMPC/DMPG/cholesterol. Both vesicle types also contained 1% fluorescence donor NBD-PE and fluorescence acceptor rhoda-mine-PE (see Materials and Methods). The graphs in Figure 4 depict the net FRET efficiency calculated at specific time points following incubation of these vesicles with each of the peptides examined.

The FRET data summarized in Figure 4 reveal significantly different vesicle interactions among the three peptides. More-over, a pronounced dependence of peptide-induced FRET modulation upon lipid composition is apparent in Figure 4 for all three peptides. Specifically, almost no effect upon the FRET results, in relation to control vesicles, was observed when the peptides were incubated with vesicles comprising DMPC and cholesterol but not DMPG [Figure 4A−C (−−−)]. This result,

indicating negligible interactions of the peptide aggregates with DMPC/cholesterol bilayers, underscores the importance of the negatively charged phospholipid DMPG in promoting vesicle interactions and lipid-induced fibrillation of all the three frag-ments examined.

Figure 4 demonstrates that incubation of all three peptides for several hours with the DMPC/DMPG/cholesterol vesicles resul-ted in a gradual increase in FRET efficiency [Figure 4A−C (—)], suggesting that the fibrils promoted vesicle aggregation (51). Previous studies have indeed correlated changes in FRET proper-ties with modification of lipid environments in membranes (52). While Figure 4 displays a clear kinetic modulation of the FRET data following incubation with the peptides, the differences between the peptides, however, are still apparent at all time points. Specifically, while the solid lines in panels A and B of
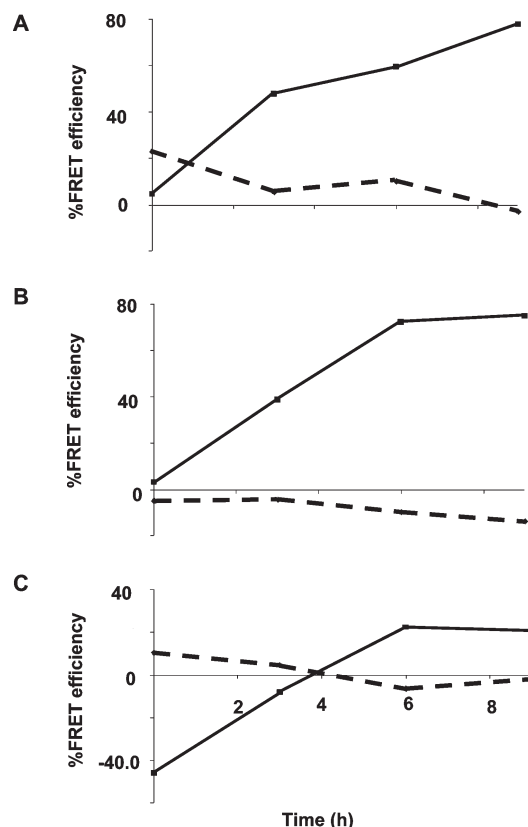
FIGURE 4: FRET modulation induced by incubation of the penta-peptides with lipid vesicles. FRET efficiency modified by preincubating the pentapeptides with NBD-PE/rhodamine-PE/DMPC/DMPG/cholesterol vesicles (—) and NBD-PE/rhodamine-PE/DMPC/cholesterol vesicles (−−−): (A) DFNKF (4 mg/mL), (B) DANKA (4 mg/mL), and (C) DFNMF (0.5 mg/mL). The FRET efficiencies are in relation to control vesicles that were not preincubated with the peptides.

Figure 4 indicate that DFNKF and DANKA, respectively, did not interfere with FRET efficiency immediately after mixing (i.e., same energy transfer occurred in the vesicles incubated with the peptides, compared to the control vesicles which were not preincubated with the peptides), DFNMF clearly disrupted the lipid bilayer upon addition to the vesicles, giving rise to significantly lower FRET [Figure 4C (—)]. Similar to the microscopy data discussed above, the FRET experiments point to different membrane interactions of DFNMF compared to the two pentapeptides containing the lysine residue instead of the methionine.

DISCUSSION

This study examines the fibrillation processes of very short peptide fragments derived from the amyloidogenic core of hCT. Short peptide models have previously provided insights into mechanistic aspects pertaining to amyloid formation (40). Furthermore, in several amyloid protein systems, it has been hypothesized that short peptide fragments essentially contain all the necessary molecular information for the formation of amyloid fibrils (53). Truncated fibril-forming peptides have been proposed, for example, as potential inhibitors of amyloid formation (54). The experiments summarized in this study underscore the significance of specific residues in affecting the fibrillation kinetics, fibril structural properties, and interaction of the peptide assemblies with lipid bilayers. Equally important, we show that the lipid composition of the vesicles significantly

affected membrane interactions of the fibrillar species formed by the three peptides studied.

The TEM data in Figure 1 demonstrate the dramatic effects upon fibril morphologies and kinetics of single-point mutations in the amyloidogenic 15−19-residue sequence of hCT, DFNKF. Specifically, lysine-to-methionine substitution considerably enhanced the fibrillation propensity and accelerated the rate of amyloidogenesis. Elucidating the factors affecting the fibrillation rate is important; rapid aggregation of overexpressed human β-amyloid protein was shown to protect mice from cognitive decline (28). Particularly striking is the observation that the mutant sequence DFNMF formed fibrils at an 8-fold lower concentration compared to the parent peptide sequence. Additionally, replacement of the positively charged lysine amino acid with the more hydrophobic and more compact methionine residue resulted in an improved lateral association of the β-sheet units, yielding substantially thicker fibrils. The morphological variations in fibril structures might point to the contribution and significance of amyloid polymorphism as a prominent factor in protein aggregation. Indeed, recent studies have underlined the close relationship between toxicity and specific structural features of amyloid aggregates (55).

Molecular dynamics simulations suggested that lysine forms a salt bridge with the C-terminus within the DFNKF fragment, contributing to stabilization of the β-sheet structure (56, 57). Our experimental data suggest, however, that hydrophobic interactions overwhelm electrostatic forces at this specific residue position. This observation can be explained by the fact that the lysine-to-methionine substitution produces an alternating pattern of hydrophobic−hydrophilic residues for the first four amino acids of DFNMF. Such a binary pattern, which maintains an amphipathic nature of parallel β-sheet aggregates, was shown to facilitate formation of supramolecular assemblies by de novo-designed peptides, regardless of their primary structures (7, 8). In agreement with the interpretation described above, the FTIR spectrum in Figure 2 shows that the DFNMF fibrils featured primarily a parallel β-sheet conformation, in contrast to other examined peptides (58).

The experimental data emphasize the significance of the two phenylalanine residues in lipid-modulated fibrillation of DFNKF. Interactions of aromatic residues were shown to play prominent roles in fibrillation of numerous amyloid proteins (59, 60). Theoretical calculations (9) and experimental approaches (10) indicated that the presence of aromatic amino acids accelerate fibrillogenesis. However, a recent study demonstrated that $\pi-\pi$ stacking is not a prerequisite for formation of fibrillar structures by the islet amyloid polypeptide (IAPP) (10). Our data similarly demonstrate that fibrillar species formed by DANKA exhibited a unique tubular morphology (Figure 1C,D). We hypothesize that substitution of the bulky aromatic residues with short-chain alanines significantly altered peptide assemblies in comparison to the native molecule, facilitating lateral growth of the fibril assemblies.

According to the FTIR spectrum in Figure 2, DANKA, in which the aromatic amino acids are absent, adopts a strictly antiparallel β-sheet fibril organization. The antiparallel arrangement of β-strands in DANKA allows more efficient interactions between adjacent β-sheets through the electrostatic attraction between aspartic acid and lysine, yielding thicker fibers. Interestingly, DANKA produced fibrils at similar or even higher rates compared to that of the native fragment. The tendency of DANKA to aggregate in aqueous solution is particularly

interesting because this fragment possesses a relatively hydrophilic sequence. The driving force for fibrillation in this case appears to be the electrostatic affinity between residues of opposite charges (i.e., aspartic acid and lysine), as well as the N- and C-termini of the peptide. The structural and kinetic data obtained for the DANKA fibrils suggest that $\pi-\pi$ stacking is not a prerequisite for fibril formation; however, aromatic interactions determine to a large extent the topology of amyloid fibrils.

The experiments highlight the impact of lipid bilayers upon the kinetics and morphology of fibril formation. TEM analysis in Figure 1 indicates that each of the three peptides studied was affected differently by DMPC/DMPG/cholesterol vesicles. While the lipid vesicles induced much faster fibrillation of both the native sequence DFNKF and the substituted peptide DFNMF, the effects of the vesicles upon the morphologies of the peptide aggregates were different. DFNKF fibrils were visually similar in vesicle-containing and vesicle-free solutions; however, the DFNMF aggregates in the presence of the vesicles appeared to be highly fragmented and uneven, compared to the smooth elongated fibrils formed in buffer. In contrast to these two peptides, fibrillation kinetics and fibril structures of DANKA were unaffected by the lipid vesicles present in the aqueous solutions.

The experiments underscore the critical roles of single residues within the short peptide fragments in the alteration of vesicle-induced fibril formation. The hydrophobic residues phenylalanine and methionine in particular appear to be central to lipid-modulated fibrillation. In this context, DANKA, in which the phenylalanines were substituted with alanines, formed aggregates after similar incubation times in buffer and in vesicle suspensions. This result stands in contrast to the results for DFNKF or DFNMF which formed fibrils much faster in the presence of lipid vesicles (Figure 1).

The CR analysis in Figure 3 illustrates the effect of lipid bilayers upon the structure and organization of fibrils formed by the three peptides. While the parent sequence DFNKF induced gold-green birefringence in buffer as well as in a vesicle suspension (Figure 3A,B), fibrils formed by the two mutants in the absence of lipids did not assemble in a similar fashion (Figure 3C,E). The mechanism of amyloid-targeted staining by CR was proposed to involve nonspecific intercalation of the dye into grooves within amyloid fibrils and binding to aromatic (*61*) and polar chemical groups (*62*). The absence of the CR green birefringence in DANKA and DFNMF assemblies formed in buffer might correspond to more rigid, compact fibrillar structures and poor accessibility of the dye to the required chemical elements.

The FRET data in Figure 4 disclose that all three peptides preferably interacted with model membranes containing negatively charged phospholipids. The FRET experiments suggest that all pentapeptides studied form membrane-active early oligomers, believed to constitute the toxic, membrane-active species, in many amyloid systems. The putative formation of prefibrillar oligomers is supported by the kinetic modulation of membrane activity apparent in Figure 4, ascribed to aggregation of oligomeric species. However, the relatively rapid fibrillation of the peptides (Figures 1 and 4) might indicate a lower abundance of prefibril oligomers. The protective effect of rapid fibrillation upon toxicity in general, the cell membrane in particular, has been recently demonstrated (*63*). The concurrent peptide-induced aggregation of the vesicles further suggests that the preformed fibrils bound at the lipid bilayer interface, thus promoting

agglomeration. While gradual vesicle aggregation was induced by all three peptides, the peptides differed in their initial membrane disruption. Specifically, the FRET data in Figure 4C demonstrate that substitution of lysine with methionine in DFNMF resulted in much more significant modulation of the bilayer organization compared to both the native sequence DFNKF as well as DANKA. This result is consistent with the pivotal role of lysine in the affinity for the negatively charged DMPG in the vesicles.

In conclusion, this work demonstrates that substitution of certain amino acids in peptide fragments significantly modifies the structural features and kinetics of fibrillar structures formed by short amyloidogenic pentapeptides. The experiments reveal that amphipathicity is an important factor not only determining the propensity to aggregate but also radically affecting fibrillar morphology. We find that aromatic interactions are not essential for fibrillation and that a zwitterionic fragment was also forming elongated tubular structures solely through electrostatic forces. Spectroscopy and microscopy data point to the interdependence of both amino acid sequence and bilayer lipid composition in determining the fibrillation kinetics and structural features of the peptide aggregates formed. Overall, this work demonstrates that amino acid sequence and lipid interactions play prominent roles in affecting aggregation processes involving even very short amyloidogenic peptide fragments.

REFERENCES

1. Ecroyd, H., and Carver, J. A. (2008) Unraveling the mysteries of protein folding and misfolding. *IUBMB Life 60*, 769–774.
2. Makin, O. S., and Serpell, L. C. (2005) Structures for amyloid fibrils. *FEBS J. 272*, 5950–5961.
3. Chiti, F., and Dobson, C. M. (2006) Protein misfolding, functional amyloid, and human disease. *Annu. Rev. Biochem. 75*, 333–366.
4. Chiti, F., Stefani, M., Taddei, N., Ramponi, G., and Dobson, C. M. (2003) Rationalization of the effects of mutations on peptide and protein aggregation rates. *Nature 424*, 805–808.
5. DuBay, K. F., Pawar, A. P., Chiti, F., Zurdo, J., Dobson, C. M., and Vendruscolo, M. (2004) Prediction of the absolute aggregation rates of amyloidogenic polypeptide chains. *J. Mol. Biol. 341*, 1317–1326.
6. Fernandez-Escamilla, A. M., Rousseau, F., Schymkowitz, J., and Serrano, L. (2004) Prediction of sequence-dependent and mutational effects on the aggregation of peptides and proteins. *Nat. Biotechnol. 22*, 1302–1306.
7. Hecht, M. H., Das, A., Go, A., Bradley, L. H., and Wei, Y. (2004) De novo proteins from designed combinatorial libraries. *Protein Sci. 13*, 1711–1723.
8. West, M. W., Wang, W., Patterson, J., Mancias, J. D., Beasley, J. R., and Hecht, M. H. (1999) De novo amyloid proteins from designed combinatorial libraries. *Proc. Natl. Acad. Sci. U.S.A. 96*, 11211–11216.
9. Tartaglia, G. G., Cavalli, A., Pellarin, R., and Caflisch, A. (2004) The role of aromaticity, exposed surface, and dipole moment in determining protein aggregation rates. *Protein Sci. 13*, 1939–1941.
10. Marek, P., Abedini, A., Song, B., Kanungo, M., Johnson, M. E., Gupta, R., Zaman, W., Wong, S. S., and Raleigh, D. P. (2007) Aromatic interactions are not required for amyloid fibril formation by islet amyloid polypeptide but do influence the rate of fibril formation and fibril morphology. *Biochemistry 46*, 3255–3261.
11. Bauer, H. H., Aebi, U., Haner, M., Hermann, R., Muller, M., and Merkle, H. P. (1995) Architecture and polymorphism of fibrillar supramolecular assemblies produced by in vitro aggregation of human calcitonin. *J. Struct. Biol. 115*, 1–15.
12. Kodali, R., and Wetzel, R. (2007) Polymorphism in the intermediates and products of amyloid assembly. *Curr. Opin. Struct. Biol. 17*, 48–57.

13. Paravastu, A. K., Leapman, R. D., Yau, W. M., and Tycko, R. (2008) Molecular structural basis for polymorphism in Alzheimer's β-amyloid fibrils. *Proc. Natl. Acad. Sci. U.S.A. 105*, 18349–18354.

14. Petkova, A. T., Leapman, R. D., Guo, Z., Yau, W. M., Mattson, M. P., and Tycko, R. (2005) Self-propagating, molecular-level polymorphism in Alzheimer's β-amyloid fibrils. *Science 307*, 262–265.

15. Zerovnik, E., Skarabot, M., Skerget, K., Giannini, S., Stoka, V., Jenko-Kokalj, S., and Staniforth, R. A. (2007) Amyloid fibril formation by human stefin B: Influence of pH and TFE on fibril growth and morphology. *Amyloid 14*, 237–247.

16. Bravo, R., Arimon, M., Valle-Delgado, J. J., Garcia, R., Durany, N., Castel, S., Cruz, M., Ventura, S., and Fernandez-Busquets, X. (2008) Sulfated polysaccharides promote the assembly of amyloid β(1−42) peptide into stable fibrils of reduced cytotoxicity. *J. Biol. Chem. 283*, 32471–32483.

17. Kim, J., Myung, E. K., Lee, I. H., and Paik, S. R. (2007) Control of morphology and subsequent toxicity of Aβ amyloid fibrils through the Dequalinium-induced seed modification. *Bull. Korean Chem. Soc. 28*, 2283–2287.

18. McLaurin, J., Yang, D., Yip, C. M., and Fraser, P. E. (2000) Review: Modulating factors in amyloid-β fibril formation. *J. Struct. Biol. 130*, 259–270.

19. Van Raaij, M. E., Segers-Nolten, I. M., and Subramaniam, V. (2006) Quantitative morphological analysis reveals ultrastructural diversity of amyloid fibrils from α-synuclein mutants. *Biophys. J. 91*, L96–L98.

20. Ambroggio, E. E., Kim, D. H., Separovic, F., Barrow, C. J., Barnham, K. J., Bagatolli, L. A., and Fidelio, G. D. (2005) Surface Behavior and Lipid Interaction of Alzheimer β-Amyloid Peptide 1−42: A Membrane-Disrupting Peptide. *Biophys. J. 88*, 2706–2713.

21. Yip, C. M., and McLaurin, J. (2001) Amyloid-β Peptide Assembly: A Critical Step in Fibrillogenesis and Membrane Disruption. *Biophys. J. 80*, 1359–1371.

22. Zhao, H., Tuominen, E. K. J., and Kinnunen, P. K. J. (2004) Formation of Amyloid Fibers Triggered by Phosphatidylserine-Containing Membranes. *Biochemistry 43*, 10302–10307.

23. Gellermann, G. P., Appel, T. R., Tannert, A., Radestock, A., Hortschansky, P., Schroeckh, V., Leisner, C., Ltkepohl, T., Shtrasburg, S., Ricken, C., Pras, M., Linke, R. P., Diekmann, S., and Faundrich, M. (2005) Raft lipids as common components of human extracellular amyloid fibrils. *Proc. Natl. Acad. Sci. U.S.A. 102*, 6297–6302.

24. McLaurin, J., and Chakrabartty, A. (1996) Membrane Disruption by Alzheimer β-Amyloid Peptides Mediated through Specific Binding to Either Phospholipids or Gangliosides. *J. Biol. Chem. 271*, 26482–26489.

25. Cordy, J. M., Cordy, J. M., Hooper, N. M., and Turner, A. J. (2006) The involvement of lipid rafts in Alzheimer's disease. *Mol. Membr. Biol. 23*, 111–122.

26. Bucciantini, M., Giannoni, E., Chiti, F., Baroni, F., Formigli, L., Zurdo, J., Taddei, N., Ramponi, G., Dobson, C. M., and Stefani, M. (2002) Inherent toxicity of aggregates implies a common mechanism for protein misfolding diseases. *Nature 416*, 507–511.

27. Caughey, B., and Lansbury, P. T. (2003) Protofibrils, pores, fibrils, and neurodegeneration: Separating the responsible protein aggregates from the innocent bystanders. *Annu. Rev. Neurosci. 26*, 267–298.

28. Cheng, I. H., Scearce-Levie, K., Legleiter, J., Palop, J. J., Gerstein, H., Bien-Ly, N., Puolivali, J., Lesne, S., Ashe, K. H., Muchowski, P. J., and Mucke, L. (2007) Accelerating amyloid-β fibrillization reduces oligomer levels and functional deficits in Alzheimer disease mouse models. *J. Biol. Chem. 282*, 23818–23828.

29. Kayed, R., Head, E., Thompson, J. L., McIntire, T. M., Milton, S. C., Cotman, C. W., and Glabe, C. G. (2003) Common Structure of Soluble Amyloid Oligomers Implies Common Mechanism of Pathogenesis. *Science 300*, 486–489.

30. Lesne, S., Koh, M. T., Kotilinek, L., Kayed, R., Glabe, C. G., Yang, A., Gallagher, M., and Ashe, K. H. (2006) A specific amyloid-β protein assembly in the brain impairs memory. *Nature 440*, 352–357.

31. Roan, N. R., Munch, J., Arhel, N., Mothes, W., Neidleman, J., Kobayashi, A., Smith-McCune, K., Kirchhoff, F., and Greene, W. C. (2009) The Cationic Properties of SEVI Underlie Its Ability To Enhance Human Immunodeficiency Virus Infection. *J. Virol. 83*, 73–80.

32. Nanga, R. P. R., Brender, J., Xu, J., Veglia, G., and Ramamoorthy, A. (2008) Structures of Rat and Human Islet Amyloid Polypeptide IAPP1−19 in Micelles by NMR Spectroscopy. *Biochemistry 47*, 12689–12697.

33. MacIntyre, I. (1967) Calcitonin: A general review. *Calcif. Tissue Res. 1*, 173–182.

34. Sletten, K., Westermark, P., and Natvig, J. B. (1976) Characterization of amyloid fibril proteins from medullary carcinoma of the thyroid. *J. Exp. Med. 143*, 993–998.

35. Arvinte, T., Cudd, A., and Drake, A. F. (1993) The structure and mechanism of formation of human calcitonin fibrils. *J. Biol. Chem. 268*, 6415–6422.

36. Wagner, K., Van Mau, N., Boichot, S., Kajava, A. V., Krauss, U., Le Grimellec, C., Beck-Sickinger, A., and Heitz, F. (2004) Interactions of the Human Calcitonin Fragment 9−32 with Phospholipids: A Monolayer Study. *Biophys. J. 87*, 386–395.

37. Diociaiuti, M., Polzi, L. Z., Valvo, L., Malchiodi-Albedi, F., Bombelli, C., and Gaudiano, M. C. (2006) Calcitonin forms oligomeric pore-like structures in lipid membranes. *Biophys. J. 91*, 2275–2281.

38. Wang, S. S., Good, T. A., and Rymer, D. L. (2005) The influence of phospholipid membranes on bovine calcitonin peptide's secondary structure and induced neurotoxic effects. *Int. J. Biochem. Cell Biol. 37*, 1656–1669.

39. Reches, M., Porat, Y., and Gazit, E. (2002) Amyloid fibril formation by pentapeptide and tetrapeptide fragments of human calcitonin. *J. Biol. Chem. 277*, 35475–35480.

40. Gazit, E. (2005) Mechanisms of amyloid fibril self-assembly and inhibition. Model short peptides as a key research tool. *FEBS J. 272*, 5971–5978.

41. Zanuy, D., Ma, B., and Nussinov, R. (2003) Short peptide amyloid organization: Stabilities and conformations of the islet amyloid peptide NFGAIL. *Biophys. J. 84*, 1884–1894.

42. Michonova-Alexova, E. I., and Sugar, I. P. (2002) Component and State Separation in DMPC/DSPC Lipid Bilayers: A Monte Carlo Simulation Study. *Biophys. J. 83*, 1820–1833.

43. Riske, K. A., Amaral, L. Q., and Lamy-Freund, M. T. (2001) Thermal transitions of DMPG bilayers in aqueous solution: SAXS structural studies. *Biochim. Biophys. Acta 1511*, 297–308.

44. Pelton, J. T., and McLean, L. R. (2000) Spectroscopic Methods for Analysis of Protein Secondary Structure. *Anal. Biochem. 277*, 167–176.

45. Castelletto, V., Hamley, I. W., and Harris, P. J. F. (2008) Self-assembly in aqueous solution of a modified amyloid β peptide fragment. *Biophys. Chem. 138*, 29–35.

46. Rojas Quijano, F. A., Morrow, D., Wise, B. M., Brancia, F. L., and Goux, W. J. (2006) Prediction of Nucleating Sequences from Amyloidogenic Propensities of Tau-Related Peptides. *Biochemistry 45*, 4638–4652.

47. Zurdo, J., Guijarro, J. I., and Dobson, C. M. (2001) Preparation and characterization of purified amyloid fibrils. *J. Am. Chem. Soc. 123*, 8141–8142.

48. Krysmann, M. J., Castelletto, V., McKendrick, J. E., Clifton, L. A., Hamley, I. W., Harris, P. J. F., and King, S. M. (2008) Self-Assembly of Peptide Nanotubes in an Organic Solvent. *Langmuir 24*, 8158–8162.

49. Howie, A. J., and Brewer, D. B. (2009) Optical properties of amyloid stained by Congo red: History and mechanisms. *Micron 40*, 285–301.

50. Clegg, R. M. (1995) Fluorescence resonance energy transfer. *Curr. Opin. Biotechnol. 6*, 103–110.

51. Loura, L. M. S., Coutinho, A., Silva, A., Fedorov, A., and Prieto, M. (2006) Structural Effects of a Basic Peptide on the Organization of Dipalmitoylphosphatidylcholine/Dipalmitoylphosphatidylserine Membranes: A Fluorescent Resonance Energy Transfer Study. *J. Phys. Chem. B 110*, 8130–8141.

52. Ishii, M., Ikushima, M., and Kurachi, Y. (2005) In vivo interaction between RGS4 and calmodulin visualized with FRET techniques: Possible involvement of lipid raft. *Biochem. Biophys. Res. Commun. 338*, 839–846.

53. Reches, M., and Gazit, E. (2004) Amyloidogenic hexapeptide fragment of medin: Homology to functional islet amyloid polypeptide fragments. *Amyloid 11*, 81–89.

54. Tjernberg, L. O., Naslund, J., Lindqvist, F., Johansson, J., Karlstrom, A. R., Thyberg, J., Terenius, L., and Nordstedt, C. (1996) Arrest of β-amyloid fibril formation by a pentapeptide ligand. *J. Biol. Chem. 271*, 8545–8548.

55. Campioni, S., Mannini, B., Zampagni, M., Pensalfini, A., Parrini, C., Evangelisti, E., Relini, A., Stefani, M., Dobson, C. M., Cecchi, C., and Chiti, F. (2010) A causative link between the structure of aberrant protein oligomers and their toxicity. *Nat. Chem. Biol. 6 (2)*, 140–147.

56. Haspel, N., Zanuy, D., Ma, B., Wolfson, H., and Nussinov, R. (2005) A comparative study of amyloid fibril formation by residues 15−19 of the human calcitonin hormone: A single β-sheet model with a small hydrophobic core. *J. Mol. Biol. 345*, 1213–1227.

57. Tsai, H. H., Zanuy, D., Haspel, N., Gunasekaran, K., Ma, B., Tsai, C. J., and Nussinov, R. (2004) The stability and dynamics of the human calcitonin amyloid peptide DFNKF. *Biophys. J. 87*, 146–158.

58. Gordon, D. J., Balbach, J. J., Tycko, R., and Meredith, S. C. (2004) Increasing the amphiphilicity of an amyloidogenic peptide changes the β-sheet structure in the fibrils from antiparallel to parallel. *Biophys. J. 86*, 428–434.

59. Gazit, E. (2002) A possible role for π-stacking in the self-assembly of amyloid fibrils. *FASEB J. 16*, 77–83.

60. Porat, Y., Stepensky, A., Ding, F. X., Naider, F., and Gazit, E. (2003) Completely different amyloidogenic potential of nearly identical peptide fragments. *Biopolymers 69*, 161–164.

61. Stains, C. I., Mondal, K., and Ghosh, I. (2007) Molecules that target β-amyloid. *ChemMedChem 2*, 1674–1692.

62. Roterman, I., KrUl, M., Nowak, M., Konieczny, L., Rybarska, J., Stopa, B., Piekarska, B., and Zemanek, G. (2001) Why Congo red binding is specific for amyloid proteins: Model studies and a computer analysis approach. *Med. Sci. Monit. 7*, 771–784.

63. Douglas, M., Fowler, A. V. K., Balch, W. E., and Kelly, J. W. (2007) Functional amyloid: From bacteria to humans. *Trends Biochem. Sci. 32* (5), 217–224.